Available online at www.sciencedirect.com
ScienceDirect
Journal of Photochemistry and Photobiology A: Chemistry 188 (2007) 317–324
Journal of Photochemistry and Photobiology A:Chemistry
www.elsevier.com/locate/jphotochem

Tyrosine groups enhance photoinduced intramolecular electron transfer in polypyridyl ruthenium(II) complexes

Yongqian Xu, Shiguo Sun, Jiangli Fan, Xiaojun Peng *

State Key Laboratory of Fine Chemicals, Dalian University of Technology,158 Zhongshan Road, Dalian 116012, PR China

Received 13 May 2006; received in revised form 13 November 2006; accepted 19 December 2006
Available online 27 December 2006

Abstract

The complexes [*cis*-$Ru^{II}L'_2(SCN)_2$ and *cis*-$Ru^{II}LL'(SCN)_2$] (L = 4,4′-bis(ethoxycarbonyl)-2,2′-bipyridine, L′ = 2,2′-bpy-4,4′-CONH-L-tyrosine ethyl ester) are prepared and characterized. Two or four tyrosine ethyl ester groups are covalently linked to a ruthenium polypyridyl photosensitizer as electron donor. Upon light excitation, intermolecular electron transfer from the excited ruthenium(II) to MV^{2+} occurs, followed by intramolecular electron transfer from tyrosine moieties to Ru(III) with a rate constant of $k_f > 1 \times 10^8\ s^{-1}$ ($\tau_f < 10$ ns).

Keywords: Ruthenium polypyridyl complexes; Tyrosine; Electron transfer; Electron donor; Photosensitizer; Photosynthesis

1. Introduction

Photoinduced electron transfer reactions are the fundamental processes in photosystem II (PS II) [1–3], where sunlight is converted into chemical energy via a photoinduced charge separated state [4]. In PS II, the electron transfer is mediated by a phenolic unit in tyrosine Z, which can avoid the quenching of the excited state of chlorophyll unit, yet ensures rapid electron transfer to P_{680}^+ [5]. In recent years, artificial model systems based on tyrosine-ruthenium-tri-bipyridine (Ru(II)(bpy)$_3$) have been studied to mimic the electron transfer reactions of PS II. It has been known that excited (Ru(II)(bpy)$_3$)* releases an electron to an intermolecular electron-acceptor (such as methyl viologen or Co^{3+}) and turns to be Ru(III)(bpy)$_3$ which could be reduced by another electron from the attached tyrosine via intramolecular electron transfer [7–10]. The rate constant of electron transfer from tyrosine to ruthenium is pH dependence. When pH is less than the pK_a of phenolic-group in tyrosine (pK_a = 10), the rate constant goes up by pH till pH > pK_a with a 100-fold great increase. However, the rate constant is still less than $10^7\ s^{-1}$. In nature the rate constant of P_{680}^+ reduced by tyrosine Z is in nanoseconds [11], and the charge-separation efficiency is close to unity [6–9]. The limited rate constant of electron transfer in artificial system may be due to the fact that there is only one tyrosine attached on ruthenium-tri-bipyridine, while in nature there is a tyrosine D besides tyrosine Z [12]. Jeans et al. studied the reduction of P_{680}^+ in PS II when tyrosine D was replaced by phenylalanine and the results showed that tyrosine D has a significant influence on electron transfer events in the vicinity of tyrosine Z [13].

Herein, two or four tyrosine groups are introduced to the ruthenium bipyridyl complexes, *cis*-$Ru^{II}L'_2(SCN)_2$ (Ru1) and *cis*-$Ru^{II}LL'(SCN)_2$ (Ru2) (L = 4,4′-bis(ethoxycarbonyl)-2,2′-bipyridine, L′ = 2,2′-bpy-4,4′-CONH-L-tyrosine ethyl ester, Scheme 1), to mimic the tyrosine Z and tyrosine D in photosystem II. The N3 dye (well-known dye used in Graetzel solar cells) is selected to meet the requirement for panchromatic absorbance [14–16]. The results show that it is much more important to speed up the photoinduced electron transfer that introducing poly-tyrosine ethyl ester side chains to the bipyridyl rings to mimic the tyrosine Z and tyrosine D in photosystem II.

2. Experiments

2.1. Materials and instruments

The chemicals used in study were reagent grade or better, and were used without further purification. Solvents were purified according to the published methods. The ligand 4,4′-dimethyl-2,2′-bipyridine (dmbpy), $RuCl_3 \cdot 3H_2O$, L-tyrosine ethyl ester

* Corresponding author. Tel.: +86 411 8899 3899; fax: +86 411 8899 3906.
E-mail address: pengxj@dlut.edu.cn (X. Peng).

1010-6030/$ – see front matter © 2006 Elsevier B.V. All rights reserved.
doi:10.1016/j.jphotochem.2006.12.029

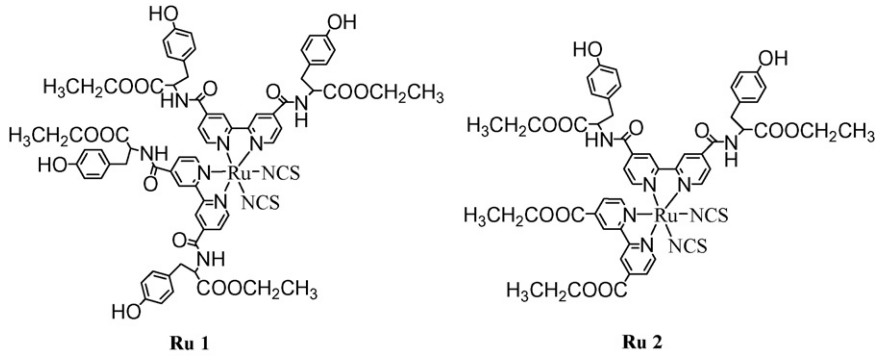

Scheme 1. Chemical structures of Ru1 and Ru2.

hydrochloride were purchased as reagent grade material from Aldrich and were used without further purification.

^{1}H NMR spectra were recorded on a Varian INOVA 400 MHz spectrometer, using TMS as internal standard. Proton assignments are based on 2D NMR (^{1}H–^{1}H COSY, HMQC and HMBC) spectra. The electro-spray ionization mass spectrometry (ESI-MS) was performed on a HP 1100LC/MS with acetonitrile as solvent. The absorption and emission measurements were performed at room temperature in air saturated acetonitrile of spectroscopic grade. The absorption spectra were recorded on a HP 8453 spectrophotometer and the emission spectra were recorded by a PTI-C-700 fluorometer. Fluorescence quantum yield was determined in ethanol solutions of rhodamine B ($\Phi_f = 0.97$) as standard at an excitation wavelength of 535 nm. Transient absorption and emission measurements were carried out using a LP 920 nanosecond laser flash photolysis. The electrochemical measurements were performed under nitrogen atmosphere and electrolyte used was 0.1 mol/L tetrabuthylammonium hexafluorophosphate ($TBAPF_6$) in acetonitrile. Cyclic voltammetry was recorded using a three-electrode system consisting of a Ag/Ag^+ (0.01 mol/L $AgNO_3$, 0.1 mol/L $TBAPF_6$, CH_3CN) as reference electrode, a platinum wire as counter electrode and a freshly polished glass carbon (diameter 2 mm) as working electrode. All potentials reported here are referenced by the Fc^+/Fc couple potential (0.080 versus Ag/Ag^+). The basic solution for all measurements was NaOH–H_2O–CH_3CN (0.1 mol/L NaOH:acetonitrile = 1:100 in volume), and the acidic solution for all measurements was HCl–H_2O–CH_3CN (0.1 mol/L HCl:acetonitrile = 1:100 in volume). Ru3 was synthesized for reference.

2.2. Synthesis

4,4′-Dicarboxyl-2,2′-bipyridine (2): As shown in Scheme 2, this compound was prepared according to the literature [17]. ^{1}H NMR (400 MHz, DMSO-d_6): δ 7.90 (d, $J = 4.8$ Hz, 2H, H_5, $H_{5'}$), 8.83 (s, 2H, H_3, $H_{3'}$), 8.90 (m, 2H, H_6, $H_{6'}$).

4,4′-Bis(ethoxycarbonyl)-2,2′-bipyridine (L): The powder of 2 (0.35 g, 1.43 mmol) was suspended in a solution of 20 mL absolute ethanol and 0.8 mL of concentrated H_2SO_4 and refluxed for 10 h, then the solution was cooled to room temperature and poured into a mixture of ice/water. Twenty-five percentage of aqueous NaOH solution was added under vigorous stirring until the solution became neutral, the white solid precipitate was collected by filtration, washed thoroughly with water and dried to give crude (L). The product was recrystallized twice from 95% ethanol, yielding 0.40 g (93%) of white needle crystals with melting point of 160–161 °C. ^{1}H NMR (400 MHz, DMSO-d_6): δ ppm 1.40 (t, 6H, $J = 7.0$ Hz, $-OCH_2CH_3$), 4.42 (q, 4H, $J = 7.0$ Hz, $-OCH_2CH_3$), 7.89 (d, 2H, $J = 4.5$ Hz, H_5, $H_{5'}$), 8.82 (s, 2H, H_3, $H_{3'}$), 8.89 (d, 2H, $J = 4.5$ Hz, H_6, $H_{6'}$). ESI-MS spectrometry of L from acetonitrile gave a peak at m/z 301.1 (calculated for $[M + H^+]$, 301.1).

2,2′-bpy-4,4′-CONH-L-tyrosine ethyl ester (L′): 2 (663 mg, 3.1 mmol) and thionyl chloride (60 mL) were heated to reflux for 4 h. After the excess thionyl chloride was evaporated, a white solid remained in the flask, and it was dried under vacuum at 60 °C for 2 h. The solid was dissolved in dry acetonitrile, and the solution was dropped into another acetonitrile solution containing L-tyrosine ethyl ester hydrochloride (1690 mg, 6.8 mmol) and triethylamine (2.0 mL) at room temperature within 20 min. The mixture was refluxed for another 4 h. After the solution

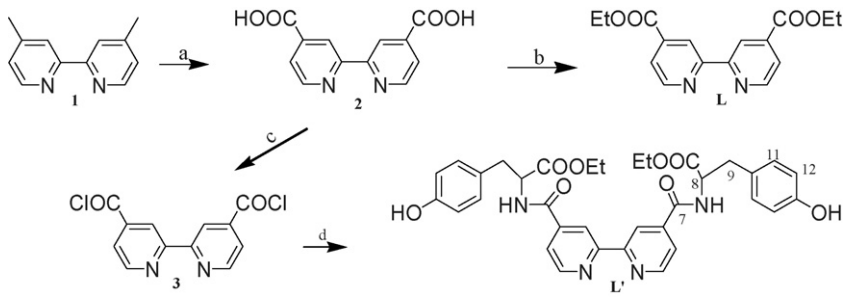

Scheme 2. Synthesis of ligand L and L′. (a) H_2SO_4, CrO_3; (b) H_2SO_4, EtOH; (c) $SOCl_2$; (d) tyrosine ethyl ester hydrochloride, Et_3N, MeCN.

was cooled to room temperature, white crystals (triethylamine hydrochloride) formed. After the crystals were filtered off, the filtrate was concentrated to near dryness, and the residue was redissolved in dichloromethane and washed three times with 0.1 M hydrochloric acid. The organic phase was dried over anhydrous sodium sulfate and evaporated to dryness, crude products were purified by column chromatography on silica gel (MeOH/$CHCl_3$ 5/95), and white crystals of L′ were obtained (yield 49%). ^{1}H NMR (δ ppm, DMSO-d_6) 1.20 (t, J = 7.0 Hz, 6H, –OCH_2CH_3), 3.01–3.07 (m, 4H, H_9, $H_{9'}$), 4.12 (q, J = 7.0 Hz, 4H, –OCH_2CH_3), 4.64 (m, 4H, H_8, $H_{8'}$), 6.65 (d, J = 8.4 Hz, 4H, H_{12}, $H_{12'}$), 7.07 (d, J = 8.4 Hz, 4H, H_{11}, $H_{11'}$), 7.78 (dd, J = 5.0 Hz, 1.0 Hz, 2H, H_5, $H_{5'}$), 8.77 (s, 2H, H_3, $H_{3'}$), 8.83 (d, J = 5.0 Hz, 2H, H_6, $H_{6'}$), 8.99 (s, 2H, –OH), 9.11 (d, J = 7.6 Hz, 2H, –NH_2), ^{13}C NMR (δ ppm, DMSO-d_6), 13.85 (–OCH_2CH_3), 35.52 (C_9), 54.49 (C_8), 60.26 (–OCH_2CH_3), 114.78 (C_{12}, $C_{12'}$), 118.26 (C_3, $C_{3'}$), 121.57 (C_5, $C_{5'}$), 127.01 (C_{10}, $C_{10'}$), 129.50 (C_{11}, $C_{11'}$), 141.95 (C_4, $C_{4'}$), 149.34 (C_6, $C_{6'}$), 155.30 (C_2, $C_{2'}$), 155.67 (C_{13}, $C_{13'}$), 164.48 (C_7, $C_{7'}$), 170.89 (–COO–). ESI-MS spectrometry of L′ from acetonitrile gave a peak at m/z 627.0 (calculated for [M + H^+], 627.0).

cis-$Ru^{II}L'_2(SCN)_2$ (Ru1): This compound was prepared according to the literature [6]. 0.229 mmol $RuCl_3 \cdot 3H_2O$ and 0.463 mmol of ligand L′ were dissolved in 20 mL DMF and refluxed under Ar for 8 h. After cooling, traces of RuL'_3 were filtered. Most of DMF solvent was evaporated under vacuum, and *cis*-$Ru^{II}L'_2Cl_2$ was precipitated with acetone and filtered. 0.428 mg of crude *cis*-$Ru^{II}L'_2Cl_2$ was dissolved in 30 mL DMF under Ar. Sodium thiocyanate (350 mg, 4.52 mmol) dissolved in 2 mL of H_2O subsequently was added to above solution. The reaction mixture was then refluxed for 6 h under Ar with magnetic stirring. Then the solvent was removed on a rotary evaporator. Crude products were purified by column chromatography on silica gel (MeOH/$CHCl_3$ 5/95) and dark red product was obtained (yield 13.4%). ^{1}H NMR (δ ppm, acetone-d_6): 1.18–1.22 (tt, J = 7.2 Hz, 12H, –OCH_2CH_3), 2.95–3.18 (qq, J = 5.6 Hz, 4H, H_9), 3.13–3.10 (qq, J = 5.6 Hz, 4H, $H_{9'}$), 4.10–4.16 (qq, J = 7.2 Hz, 4H, –OCH_2CH_3), 4.22 (q, J = 6.8 Hz, 4H, –OCH_2CH_3), 4.78–4.79 (m, 2H, H_8), 4.94–4.96 (m, 2H, $H_{8'}$), 6.74 (dd, J = 8.4 Hz, J = 8.8 Hz, 4H, H_{12}), 6.84 (d, J = 8.8 Hz, 4H, $H_{12'}$), 7.12 (t, J = 7.6 Hz, 4H, H_{11}), 7.30 (t, J = 8.0 Hz, 4H, $H_{11'}$), 7.47 (d, J = 6.0 Hz, 2H, H_5), 7.95 (d, J = 6.0 Hz, 2H, H_6), 8.24 (dd, J = 7.2 Hz, J = 0.3 Hz, 2H, $H_{6'}$), 8.30 (d, J = 6.0 Hz, 2H, $H_{5'}$), 8.82 (d, J = 22.8 Hz, 2H, H_3), 8.93 (d, J = 16.0 Hz, 2H, $H_{3'}$); ^{13}C NMR (δ ppm, acetone-d_6): 13.80 (–OCH_2CH_3), 36.60 (C_9, $C_{9'}$), 55.20 (C_8, $C_{8'}$), 61.18 (–OCH_2CH_3), 115.54 (C_{12}, $C_{12'}$), 121.05 (C_3), 121.44 ($C_{3'}$), 123.88 (C_5), 124.59 ($C_{5'}$), 127.85 (C_{10}, $C_{10'}$), 130.53 (C_{11}, $C_{11'}$), 132.74 (C of NCS), 133.59 (C of NCS′), 140.55 (C_4), 141.28 ($C_{4'}$), 153.17 (C_6), 153.71 ($C_{6'}$), 156.59 (C_{13}, $C_{13'}$), 157.89 (C_2), 159.32 ($C_{2'}$), 163.87 (C_7, $C_{7'}$), 171.35 (–COO–). ESI-MS spectrometry of Ru1 from acetonitrile gave a monocharged peak at m/z 1494.2 (calculated for [M + Na^+], 1494.2).

cis-$Ru^{II}LL'(SCN)_2$ (Ru2): $RuCl_3 \cdot 3H_2O$ (0.5 g, 2 mmol), dissolved in dry DMF (35 mL), was treated with an excess of anhydrous LiCl (0.2 g, 4.7 mmol) to give a suspension which was stirred for 5 min at 90 °C. Ligand L′ (2.2 mmol), dissolved in DMF (20 mL), was added to this solution, and the mixture was then stirred for 6 h under a nitrogen atmosphere. Then the solution was gradually warmed to 110 °C before L (2.4 mmol) was added, and the resulting mixture was stirred under nitrogen for an additional 10 h. After being cooled to room temperature, the solution was filtered to remove a small amount of unreacted ruthenium(III) chloride and other insoluble components. Sodium thiocyanate (23 mmol) dissolved in 2 mL of H_2O subsequently was added to the above solution. The reaction mixture was refluxed for 6 h under Ar with magnetic stirring. Then the solvent was removed on a rotary evaporator. Crude products were purified by column chromatography on silica gel (MeOH/$CHCl_3$ 3/97) and dark red product was obtained (yield 7.3%). ^{1}H NMR (δ ppm, acetone-d_6): 1.17–1.20 (tt, J = 7.2 Hz, 6H, tyr-OCH_2CH_3), 1.35 (t, J = 7.2 Hz, 3H, –OCH_2CH_3), 1.50 (t, J = 7.2 Hz, 3H, –OCH_2CH_3), 3.00–3.17 (qq, J = 14.0 Hz, 2H, H_9), 3.12–3.29 (qq, J = 14.0 Hz, 2H, $H_{9'}$), 4.17 (q, J = 7.2 Hz, 2H, tyr-OCH_2CH_3), 4.22 (q, J = 7.2 Hz, 2H, tyr-OCH_2CH_3), 4.40 (q, J = 7.2 Hz, 2H, –OCH_2CH_3), 4.57 (q, J = 7.2 Hz, 2H, –OCH_2CH_3), 4.77–4.81 (m, 1H, H_7), 4.94–4.97 (m, 1H, $H_{7'}$), 6.74 (q, J = 8.0 Hz, 2H, H_{12}), 6.84 (dd, J = 8.8 Hz, J = 2.4 Hz, 2H, $H_{12'}$), 7.11 (t, J = 8.4 Hz, 2H, H_{11}), 7.25 (dd, J = 11.6 Hz, J = 8.8 Hz, 2H, $H_{11'}$), 7.49 (d, J = 5.6 Hz, 1H, H_5), 7.63 (d, J = 6.0 Hz, 1H, 4,4′-di-$COOCH_2CH_3$-bpy-H_5), 7.91 (t, J = 4.8 Hz, 1H, H_6), 8.06 (q, J = 2.8 Hz, 1H, 4,4′-di-$COOCH_2CH_3$-bpy-H_6), 8.20 (d, J = 6.4 Hz, 1H, 4,4′-di-$COOCH_2CH_3$-bpy-$H_{6'}$), 8.24 (d, J = 8.8 Hz, 1H, $H_{6'}$), 8.30 (d, J = 7.6 Hz,1H, $H_{5'}$), 8.37–8.39 (m, 1H, 4,4′-di-$COOCH_2CH_3$-bpy-$H_{5'}$), 8.78 (d, J = 28.4 Hz, 1H, H_3), 8.90 (d, J = 7.2 Hz, 1H, $H_{3'}$), 8.90 (s, 1H, 4,4′-di-$COOCH_2CH_3$-bpy-H_3), 9.16 (s, 1H, 4,4′-di-$COOCH_2CH_3$-bpy$H_{3'}$); ^{13}C NMR (δ ppm, acetone-d_6): 14.47 (tyr-OCH_2CH_3), 37.32 (C_9, $C_{9'}$), 55.85 (C_7, $C_{7'}$), 61.87 (tyr-OCH_2CH_3), 63.02 (–OCH_2CH_3), 116.24 (C_{12}, $C_{12'}$), 121.69 (C_3), 122.22 ($C_{3'}$), 123.23 (C_5), 123.47 ($C_{5'}$), 124.81 (4,4′-di-$COOCH_2CH_3$-bpyC_3), 125.33 (4,4′-di-$COOCH_2CH_3$-bpy$C_{3'}$), 125.79 (4,4′-di-$COOCH_2CH_3$-bpyC_5), 126.73 (4,4′-di-$COOCH_2CH_3$-bpy$C_{5'}$), 128.63 (C_{10}, $C_{10'}$), 131.21 (C_{11}, $C_{11'}$), 133.86 (C of NCS), 134.12 (C of NCS′), 137.71 (4,4′-di-$COOCH_2CH_3$-bpyC_4), 138.50 (4,4′-di-$COOCH_2CH_3$-bpy$C_{4'}$), 141.61 (C_4), 142.27 ($C_{4'}$), 153.72 (C_6), 154.24 ($C_{6'}$), 154.41 (4,4′-di-$COOCH_2CH_3$-bpyC_6), 154.92 (4,4′-di-$COOCH_2CH_3$-bpy$C_{6'}$), 157.33 (C_{13}, $C_{13'}$), 158.53 (C_2), 158.90 (4,4′-di-$COOCH_2CH_3$-bpyC_2), 159.80 ($C_{2'}$), 160.37 (4,4′-di-$COOCH_2CH_3$-bpy$C_{2'}$), 164.26 (–COO–), 164.68 (C_7, $C_{7'}$), 171.92 (tyr-COO–). ESI-MS spectrometry of Ru1 from acetonitrile gave a monocharged peak at m/z 1167.2 (calculated for [M + Na^+]$^+$, 1167.2).

cis-$Ru^{II}L_2(SCN)_2$ (Ru3): This compound was prepared according to the synthesis of Ru1 described above. Dark red product was obtained (yield 15.2%). ^{1}H NMR (δ ppm, $CDCl_3$): 1.41 (t, J = 7.2 Hz, 6H, –OCH_2CH_3), 1.54 (t, J = 7.2 Hz, 6H, –OCH_2CH_3), 4.45 (q, J = 7.2 Hz, 4H, –OCH_2CH_3), 4.60 (q, J = 6.8 Hz, 4H, –OCH_2CH_3), 8.25 (d, J = 6.0 Hz, 4H, H_5, $H_{5'}$), 8.69 (s, 4H, H_6, $H_{6'}$), 8.85 (s, 4H, H_3, $H_{3'}$). ESI-MS spectrometry of Ru3 from acetonitrile gave a monocharged peak at m/z 841.1 (calculated for [M + Na^+], 841.1).

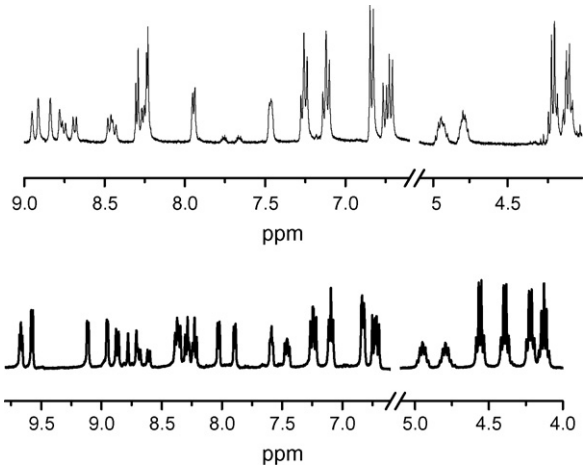

Fig. 1. ^{1}H NMR spectrum of complexes Ru1 (up) and Ru2 (bottom) in acetone-d_6. For clarity the peaks in the high magnetic region are not included.

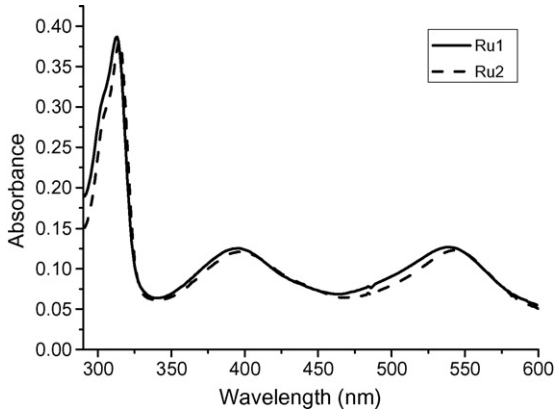

Fig. 3. UV–vis absorption spectrum of complexes Ru1 (10 μM) and Ru2 (10 μM) in acetonitrile.

3. Results and discussion

3.1. NMR spectral data

The ^{1}H NMR and ^{13}C NMR of Ru1 and Ru2 are consistent with the structures shown in Scheme 1, which are complicated because introduction of NCS ligands make pyridyl rings inequivalent concerning electronic environment. The two NCS ligands are *trans* to bipyridyl rings.

The comparison of the ^{1}H NMR spectra of the Ru1 and Ru2 complexes are shown in Fig. 1, two halves of each bipyridine ligand are in distinct magnetic environments and show 6 resonance peaks in the aromatic region corresponding to two pyridyl rings. At 4.00–4.25 ppm region, there are two groups of quartic peaks corresponding to two different –OCH_2CH$_3$ on tyrosine ligand.

In the Ru2 complex, there are two types of 2,2′-bipyridine ligands containing tyrosine ethyl ester and ethoxycarbonyl, respectively, in which one 2,2′-bipyridine is *trans* to the other and at the same time *trans* to NCS ligand. So they are in different electronic environments and show 12 resonance peaks in the aromatic region corresponding to four pyridyl rings. At 4.00–4.50 ppm region, there are four groups of quadruple peaks corresponding to two different –OCH_2CH$_3$ of tyrosine ethyl ester and two different –OCH_2CH$_3$ attached directly to bipyridine.

In Fig. 2, ^{13}C NMR spectra of the Ru1 and Ru2 complexes are compared. At 130–135 ppm, both of them have two peaks, which are corresponding to the N-coordinated thiocyanate carbon resonance peaks [17]. It indicates that NCS ligands are coordinated through the nitrogen end in both of Ru1 and Ru2. The pyridyl rings of bipyridyl ligand in Ru1 and Ru2 are in different electronic environment from the splitting peaks at 121.05 (C_3), 121.44 ($C_{3'}$) for Ru1 and the peaks at 121.69 (C_3), 122.22 ($C_{3'}$) for Ru2.

3.2. IR spectral data

The NCS ligands coordinated through the nitrogen end in Ru1 and Ru2 can be further confirmed by IR: a strong absorption in the range of 2100–2115 cm^{-1} is observed. This can be attributed to ν(NC) of the thiocyanate ligand in Ru1 and Ru2 complexes. The band at 824 cm^{-1} is due to ν(CS) of the thiocyanate ligand [15].

3.3. Absorption spectra

The absorption spectral data for two complexes are shown in Table 1 and Fig. 3. Both Ru1 and Ru2 show broad and intense visible bands between 390 nm and 540 nm, which are due to metal-to-ligand charge-transfer transitions (MLCT) [16a]. It is

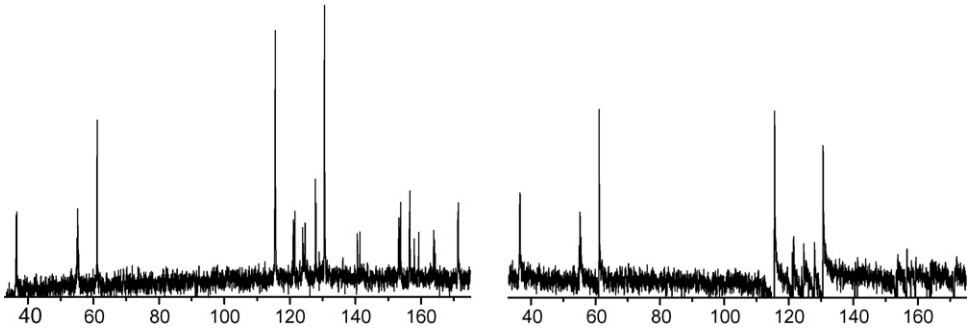

Fig. 2. ^{13}C NMR spectrum of complexes Ru1 (left) and Ru2 (right) in acetone-d_6.

Table 1
Absorption, photophysical and electrochemical properties of the ruthenium complexes

Complex	Solvent	λ_{ab} (nm) (ε, 10^4 M^{-1} cm^{-1})		Emission, λ_{em} (nm)[a]	E_p(V), $Ru^{III/II}$	E_p(V), $Tyr^{+/0}$	$E_{1/2}$(V) (ΔE_p/mV)	$E_{1/2}$(V), L	$E_{1/2}$(V), L′
		π–π^*	$d\pi$–π^*						
Ru1	(CH_3CN)[b]	313 (3.87)	396 (1.25) 539 (1.27)	801	0.63	0.86[c]	−1.45 (80) −1.68 (90)	–	−2.36[c]
Ru2	(CH_3CN)[b]	315 (3.80)	396 (1.21) 543 (1.23)	801	0.63	0.88[c]	−1.39 (80) −1.64 (80)	−2.07[c]	−2.34[c]
Ru1	(HCl)[d]	–	–	–	0.62	0.79[c]	−1.34[c] −1.48[c]	–	–
Ru2	(HCl)[d]	–	–	–	0.62	0.80[c]	−1.38[c] −1.54[c]	–	–
Ru1	(NaOH)[e]	–	–	–	0.61	0.29[c]	−1.47[c] −1.69[c]	–	−2.31[c]
Ru2	(NaOH)[e]	–	–	–	0.60	0.30[c]	−1.38[c] −1.62[c]	–	–

[a] Emission data were obtained by exciting at lowest energy MLCT band at 535 nm, in degassed acetonitrile at room temperature.
[b] Peak potential determined from DPV measurement.
[c] The electrochemical data were measured in CH_3CN solvent with 0.1 M tetrabutyl ammonium hexafluorophosphate using a glassy carbon electrode. The reported data are V vs. Ag/Ag^+. $E_{1/2} = (E_{pa} + E_{pc})/2$.
[d] The electrochemical data were measured in HCl (0.1 mol/L)–CH_3CN (v/v 1:100) acid solution.
[e] The electrochemical data were measured in NaOH (0.1 mol/L)–CH_3CN (v/v 1:100) basic solution.

in agreement with the result for the unsubstituted N3 analogues [15,16a]. The band in the UV region at 315 nm is assigned to intra ligand (π–π^*) transitions of bipyridine ligands. For both Ru1 and Ru2, the MLCT band is red-shifted by 90 nm compared to the typical MLCT band in the $Ru(bpy)_3^{2+}$ (λ_{max} at 450 nm) analogues. The red shift is resulted from the presence of the NCS ligand. The MLCT transitions of the complexes Ru1 and Ru2 involve the excitations from d-orbital (t_{2g}, HOMO) of ruthenium to π^*-orbital of bipyridine ligand. When coordinated with Ru, SCN^- will increase the energy level of the d-orbital [16b]. Therefore, the energy gap between the d-orbital and the π^*-orbital ($d\pi_M \rightarrow \pi_L{}^*$) decreases and the absorption spectra of Ru1 and Ru2 show red-shifts in the MLCT transitions. However, the absorption spectra and the extinction coefficient remain unchanged when ethoxycarbonyl groups are replaced by tyrosine ethyl ester groups.

3.4. Steady-state emission spectra

The emission spectra of Ru1 and Ru2 in degassed acetonitrile by excitation at 535 nm at room temperature are shown in Fig. 4. Fluorescence quantum yields for Ru1 and Ru2 are 1.59×10^{-3} and 1.66×10^{-3}, respectively, which indicates that the excited state of ruthenium is not quenched by tyrosine ethyl ester.

3.5. Electrochemical data

The redox properties of these complexes are studied by cyclic voltammetry (CV) and differential pulse voltammetry (DPV). The data are collected in Table 1. Half-wave potentials ($E_{1/2}$) are determined by cyclic voltammetry as the average of anodic (E_{pa}) and cathodic (E_{pc}) peak potentials ($E_{1/2} = (E_{pa} + E_{pc})/2$). For the irreversible component, half-wave potentials are determined from DPV peak potentials. Typical cyclic voltammograms of the complexes Ru1 and Ru2 in basic solution are displayed in Fig. 5.

To make an unambiguous assignment of the redox peaks for both Ru1 and Ru2, we studied complex Ru3 (Fig. 6). Three potentials at −1.33 V (70 mV), −1.55 V (80 mV), −2.03 V can be observed in Ru3. The peak at −2.03 V (in the CV of Ru3) can be assigned to the reduction of ligand L and the peak at −2.36 V (in the CV of Ru1 and Ru2) should be assigned to the reduction of ligand L′. As the similar Ru compound containing COOH groups (instead of their ester, $CO_2CH_2CH_3$) studied by Graetzel [22] did not display the peaks in the range of −1.1 to −1.6 V, we assign the peaks as the reduction of –COOEt of ligand L or L′.

The pH effect on the CV potentials of the tyrosines in Ru1 and Ru2 is in good agreement with previous reports for tyrosine [6–9,18]. Upon addition of 0.1 mol/L NaOH (6 equiv.) into the acetonitrile solution of ligand L′, the oxidation potential of L′ decreases from 0.8 V to 0.3 V (Fig. 5d), and the same phenomena

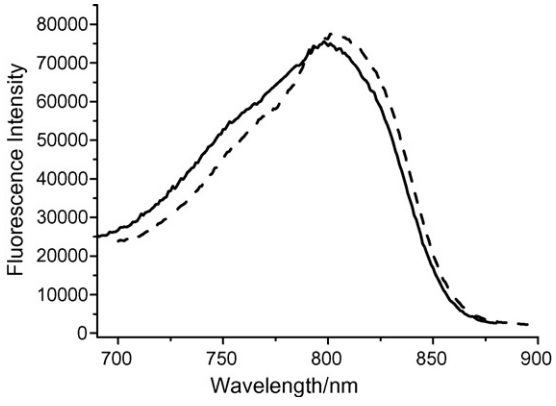

Fig. 4. The emission spectra of Ru1 (10 μM) (solid line) and Ru2 (10 μM) (dotted line) in deoxygenated acetonitrile at room temperature.

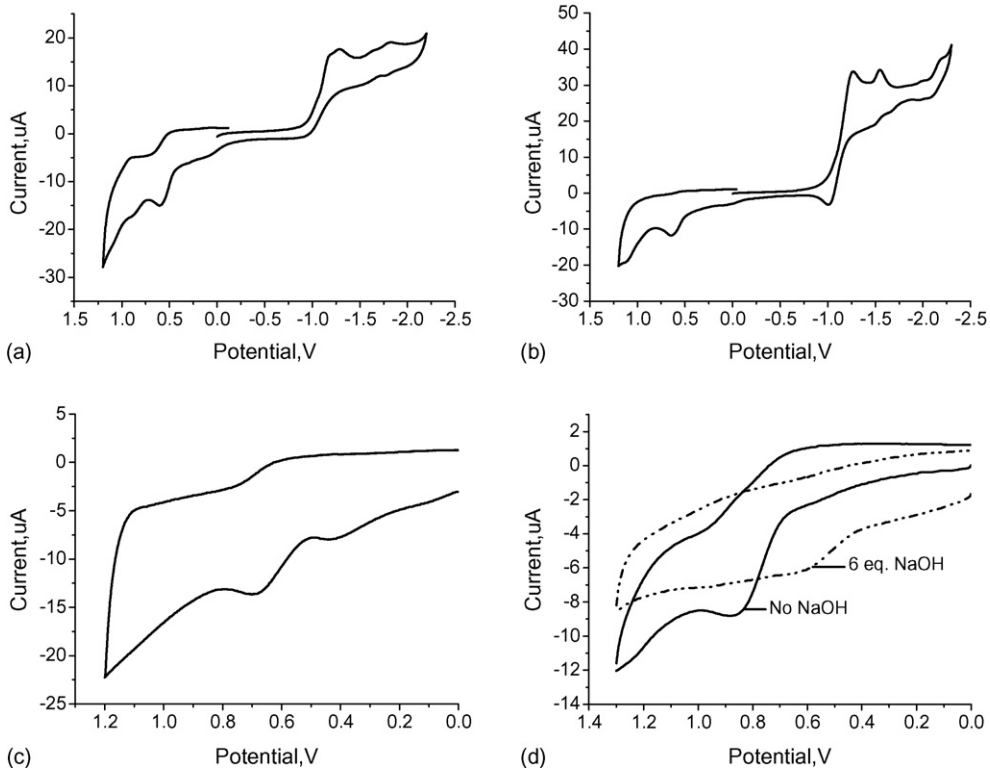

Fig. 5. The cyclic voltammograms of Ru1 (a), Ru2 (b), Ru1 partial CV in deoxygenated 10% aq. NaOH–CH_3CN (1:9 in volume) (c) and L′ in water–CH_3CN (1:9 in volume) with 0 or 6 equiv. of NaOH (d) (scan rate: 100 mV/s).

can also be observed for the complexes Ru1 and Ru2 (Table 1, Fig. 5). The potential shifts are due to the deprotonation of phenol groups. Adding HCl (0.1 mol/L) to the acetonitrile solutions of L′, Ru1 or Ru2, no obvious change can be detected in the oxidation potential range. In the whole positive potential range, the quasi-reversible couple at $E_{1/2}$ 0.63 V is assigned to the $Ru^{II/III}$ couple, and the deprotonated tyrosine phenolic oxidation peak potential is at E_p 0.3 V versus Ag/Ag^+.

The oxidation potentials of Ru1 and Ru2 (0.63 V) are lower than that of the free phenolic tyrosine (0.86–0.88 V) in neutral solution [9], in which the thermodynamically unfavorable electron transfer from the free phenolic tyrosine to Ru(III) cannot occur spontaneously. But the deprotonated phenolic groups in tyrosine show a much lower oxidation potential (0.3 V), the potential difference between the $Ru^{II/III}$ couple and the $Tyr^{ox/red}$ couple is about 0.3 V for both Ru1 and Ru2, which makes the electron transfer process thermodynamically possible.

3.6. Photoinduced electron transfer

The electron transfer from the tyrosine or deprotonated tyrosine to the oxidated Ru^{III} is triggered by the "flash-quenched method" [10–20]. About 10-fold excess of electron acceptor (methyl viologen) was added into a 1×10^{-4} mol/L complex in acetonitrile solvent. Upon excitation of Ru^{II} complex by a nanosecond laser flash at 532 nm, it is rapidly ($\tau < 1$ ns) oxidized to Ru^{III} by the external electron acceptor.

Following the decay of the Ru(II) triplet MLCT state, the transient absorption spectra show mainly the bleaching of the Ru(II) chromophore due to the formation of Ru(III) based on

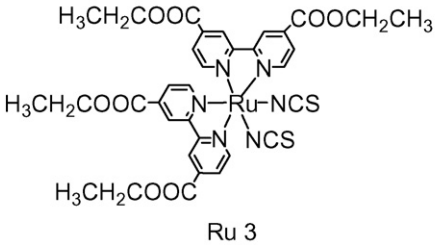

Ru 3

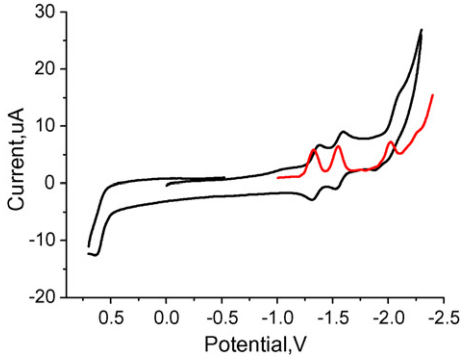

Fig. 6. DPV (in red) and the cyclic voltammogram of ligand Ru3 in deoxygenated acetonitrile (scan rate: 100 mV/s, scan scale: 0.8 V to −2.6 V).

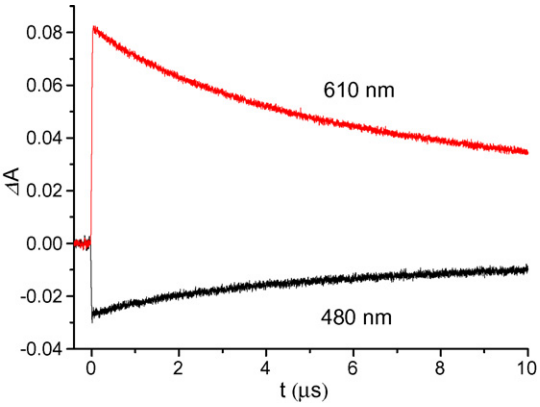

Fig. 7. Transient absorbance traces for Ru1 after a 532 nm laser flash in dry acetonitrile, showing the bleaching of the Ru^{II} at 480 nm (lower trance) and the kinetic decay of the $MV^{+\bullet}$ radical at 610 nm (upper trance).

electron transfer from the MLCT state to the electron acceptor MV^{2+}. This can be monitored with the rapid appearance of the $MV^{+\bullet}$ absorption around 610 nm.

$$[Ru^{II}\text{-TyrH}](NCS)_2 + MV^{2+} + h\nu \rightarrow [{}^*Ru^{II}\text{-TyrH}](NCS)_2 + MV^{2+} \rightarrow [Ru^{III}\text{-TyrH}](NCS)_2 + MV^{+\bullet} \leftrightarrow [Ru^{II}\text{-TyrH}](NCS)_2 + MV^{2+} \quad (1)$$

In principle, there are two possible ways for the photogenerated Ru(III) to return to the Ru(II) ground state: either by reverse electron transfer from the $MV^{+\bullet}$ (charge recombination) (Eq. (1)) or by a second intramolecular electron transfer from the linked tyrosine moiety. As the oxidation potential of tyrosine is higher than that of ruthenium(II), tyrosine does not participate in the electron transfer and does not compete with the charge recombination between the Ru(III) and the $MV^{+\bullet}$ as shown in Fig. 7, the kinetic decay rate of $MV^{+\bullet}$ is in the same level as that of Ru(III).

When the tyrosine is deprotonated, the oxidation potential of tyrosine becomes lower than that of Ru (II). In this case, the bleaching signal decays completely within a shorter time (Fig. 8), which indicates that Ru(III) generated by electron transfer is quickly reduced by the electrons not only coming from $MV^{+\bullet}$, but also from another electron donor—tyrosine, the intramolecular electron transfer successfully competes with the charge recombination.

$$[Ru^{II}\text{-Tyr}](NCS)_2 + h\nu \rightarrow [{}^*Ru^{II}\text{-Tyr}](NCS)_2$$
$$[{}^*Ru^{II}\text{-Tyr}](NCS)_2 + MV^{2+} \rightarrow [Ru^{III}\text{-Tyr}] + MV^{+\bullet} \quad (2)$$
$$[Ru^{III}\text{-Tyr}](NCS)_2 + MV^{+\bullet} \leftrightarrow [Ru^{II}\text{-Tyr}^{\bullet}](NCS)_2 + MV^{+\bullet}$$

As shown in Fig. 8, the kinetic decay of Ru(III) is much faster than that of the $MV^{+\bullet}$. Unfortunately, the kinetic decay of intramolecular electron transfer is too fast to be well detected on this nanosecond instrument (the minimum limit of detection is 10 ns), which suggests that the time scale for intramolecular electron transfer is less than 10 ns. In other word, intramolecular electron transfer from tyrosine moiety to Ru(III) takes place with a rate constant of $k_f > 1 \times 10^8\ s^{-1}$ ($\tau_f < 10$ ns). In Ru2, four tyrosine side chains are introduced, the process of photoinduced electron transfer is similar as that of Ru1 in the detectable time scale.

As the absorption of tyrosyl radical (390–420 nm) aroused by intramolecular electron transfer [21] overlaps with that of the $MV^{+\bullet}$, it cannot be observed clearly in the experiments.

The photoinduced intramolecular electron transfer rate ($k_f > 1 \times 10^8\ s^{-1}$) for Ru1 or Ru2 is much faster than that of the reported complex $Ru(bpy)_3{}^{2+}$-tyr ($k_f = 5 \times 10^4\ s^{-1}$) [10], in which only one tyrosine ethyl ester side chain was covalently linked to bipyridyl ring as electron donor. Therefore, it is a good way for introducing two or more tyrosine ethyl ester side chains to the bipyridyl rings to mimic the tyrosine Z and tyrosine D in photosystem II to increase the intramolecular electron transfer efficiency.

4. Conclusion

Two new ruthenium complexes containing two or four tyrosine ethyl ester groups were synthesized and characterized as electron donor. Upon excitation at 532 nm, photoinduced electron transfer occurred from the MLCT state to the electron acceptor MV^{2+}, then the resulting Ru(III) was reduced by the tyrosine groups through intramolecular electron transfer with a rate constant of $k_f > 1 \times 10^8\ s^{-1}$ ($\tau_f < 10$ ns). It demonstrates that introducing two or more tyrosine ethyl ester side chains to the bipyridyl rings of the ruthenium bipyridyl complex is much more efficient to speed up the photoinduced electron transfer.

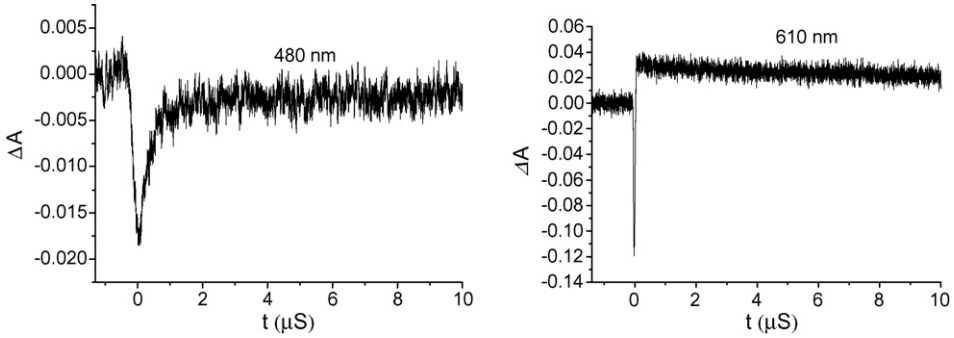

Fig. 8. Transient absorbance traces for Ru1 after a 532 nm laser flash in basic solution, showing the rapid bleaching of the Ru^{II} at 480 nm (left trace) and the slow kinetic decay of the $MV^{+\bullet}$ radical at 610 nm (right trance).

This is the first operative model to mimic both tyrosine Z and tyrosine D in photosystem II.

Acknowledgements

This work was financially supported by the Education Ministry of China and the National Natural Science Foundation of China (project 20376010 and 20472012).

Appendix A. Supplementary data

Supplementary data associated with this article can be found, in the online version, at doi:10.1016/j.jphotochem.2006.12.029.

References

[1] H. Dieks, M.O. Senge, B. Kirste, H. Kurreck, J. Org. Chem. B 62 (1997) 8666–8680.
[2] (a) R. Argazzi, C.A. Bignozzi, T.A. Heimer, F.N. Castellano, G.J. Meyer, J. Phys. Chem. B 101 (1997) 2591–2597;
(b) R. Argazzi, C.A. Bignozzi, T.A. Heimer, F.N. Castellano, G.J. Meyer, J. Am. Chem. Soc. 117 (1995) 11815–11816;
(c) C. Kleverlaan, M. Alcbbi, R. Argazzi, C.A. Bignozzi, G.M. Hasselman, G.J. Meyer, Inorg. Chem. 39 (2000) 1342–1343.
[3] P. Bonhote, J.-E. Moser, R. Humphry-Baker, N. Vlachopoulos, S.M. Zakeeruddin, L. Walder, M. Gratzel, J. Am. Chem. Soc. 121 (1999) 1324–1336.
[4] J. Barber, B. Andersson, Nature 370 (1994) 31–34.
[5] (a) C. Jeans, M.J. Schilstra, D.R. Klug, Biochemistry 41 (2002) 5015–5023;
(b) B.A. Diner, D.A. Force, D.W. Randall, R.D. Britt, Biochemistry 37 (1998) 17931–17943;
(c) M.R.A. Blomberg, P.E.M. Siegbahn, G.T. Babcock, J. Am. Chem. Soc. 120 (1998) 8812–8824.
[6] C. Tommos, X.S. Tang, K. Warncke, C.W. Hoganson, S. Styring, J. McCracken, B.A. Diner, G.T. Babcock, J. Am. Chem. Soc. 117 (1995) 10325–10335.
[7] O. Johansson, M. Borgstrom, R. Lomoth, M. Palmblad, J. Bergquist, L. Hammarstrom, L. Sun, B. Akermark, Inorg. Chem. 42 (2003) 2908–2918.
[8] R. Ghanem, Y. Xu, J. Pan, T. Hoffmann, J. Andersson, T. Polvka, T. Pascher, S. Styring, L. Sun, V. Sundstrom, Inorg. Chem. 41 (2002) 6258–6266.
[9] J. Pan, Y. Xu, G. Benko, Y. Feyziyev, S. Styring, L. Sun, B. Akermark, T. Polivka, V. Sundstrom, J. Phys. Chem. B 108 (2004) 12904–12910.
[10] A. Magnuson, H. Berglund, P. Korall, L. Hammarstrom, B. Akermark, S. Styring, L. Sun, J. Am. Chem. Soc. 119 (1997) 10720–10725.
[11] (a) G. Christen, A. Seeliger, G. Renger, Biochemistry 38 (1999) 6082–6092;
(b) J.S. Maria, R. Fabrice, H.A.N. Jonathan, J.B. Christopher, R.K. David, Biochemistry 37 (1998) 3974–3981.
[12] A. Astashkin, Y. Kodera, A. Kawamori, Biochim. Biophys. Acta 1187 (1994) 89–93.
[13] C. Jeans, M.J. Schilstra, N. Ray, S. Husain, J. Minagawa, J.H.A. Nugent, D.R. Klug, Biochemistry 41 (2002) 15754–15761.
[14] M.K. Nazeeruddin, A. Kay, I. Rodicio, R. Humphry-Baker, E. Muller, P. Liska, N. Vlachopoulos, M. Graetzel, J. Am. Chem. Soc. 115 (1993) 6382–6390.
[15] M.K. Nazeeruddin, P. Pechy, T. Renouard, S.M. Zakeeruddin, R. Humphry-Baker, P. Comte, P. Liska, L. Cevey, E. Costa, V. Shklover, L. Spiccia, G.B. Deacon, C.A. Bignozzi, M.G. Raetzel, J. Am. Chem. Soc. 123 (2001) 1613–1624.
[16] (a) K. Kalyanasundaram, M. Graetzel, Coord. Chem. Rev. 77 (1998) 347–414;
(b) A. Islam, H. Sugihara, H. Arakawa, J. Photochem. Photobiol. A: Chem. 158 (2003) 131–138.
[17] M.K. Nazeeruddin, S.M. Zakeeruddin, R. Humphry-Baker, S.I. Gorelsky, A.B.P. Lever, M. Gratzel, Coord. Chem. Rev. 208 (2000) 213–225.
[18] M. Sjodin, S. Styring, H. Wolpher, Y. Xu, L. Sun, L. Hammarstrom, J. Am. Chem. Soc. 127 (2005) 3855–3863.
[19] M. Sjodin, S. Styring, B. Akermark, L. Sun, L. Hammarstrom, J. Am. Chem. Soc. 122 (2000) 3932–3936.
[20] I.J. Chang, H.B. Gray, J.R. Winkler, J. Am. Chem. Soc. 113 (1991) 7056–7057.
[21] J. Pan, W. Lin, W. Wang, Z. Han, C. Lu, S. Yao, N. Lin, D. Zhu, Biophys. Chem. 89 (2001) 193–199.
[22] (a) Md.K. Nazeeruddin, C. Klein, P. Liska, M. Graetzel, Coord. Chem. Rev. 249 (2005) 1460–1467;
(b) Md.K. Nazeeruddin, S.M. Zakeeruddin, J.-J. Lagref, P. Liska, P. Comte, C. Barolo, G. Viscardi, K. Schenk, M. Graetzel, Coord. Chem. Rev. 248 (2004) 1317–1328;
(c) N. Hirata, J.-J. Lagref, E.J. Palomares, J.R. Durrant, M.K. Nazeeruddin, M. Gratzel, D.D. Censo, Chem. Eur. J. 10 (2004) 595–602.